ORIGINAL ARTICLE

JBMR®

^{18}F-fluoride PET as a Noninvasive Imaging Biomarker for Determining Treatment Efficacy of Bone Active Agents at the Hip: A Prospective, Randomized, Controlled Clinical Study

Michelle L Frost,[1] Amelia E Moore,[1] Musib Siddique,[1] Glen M Blake,[1] Didier Laurent,[2] Babul Borah,[2] Ursula Schramm,[2] Marie-Anne Valentin,[2] Theodore C Pellas,[2] Paul K Marsden,[3] Paul J Schleyer,[3] and Ignac Fogelman[1]

[1]Osteoporosis Screening and Research Unit, King's College London, King's Health Partners, Guy's Campus, London, United Kingdom
[2]Novartis Pharma AG, Basel, Switzerland
[3]PET Imaging Centre, King's College London, King's Health Partners, St Thomas' Campus, London, United Kingdom

ABSTRACT

The functional imaging technique of ^{18}F-fluoride positron emission tomography (^{18}F-PET) allows the noninvasive quantitative assessment of regional bone formation at any skeletal site, including the spine and hip. The aim of this study was to determine if ^{18}F-PET can be used as an early biomarker of treatment efficacy at the hip. Twenty-seven treatment-naive postmenopausal women with osteopenia were randomized to receive teriparatide and calcium and vitamin D (TPT group, $n = 13$) or calcium and vitamin D only (control group, $n = 14$). Subjects in the TPT group were treated with 20 μg/day teriparatide for 12 weeks. ^{18}F-PET scans of the proximal femur, pelvis, and lumbar spine were performed at baseline and 12 weeks. The plasma clearance of ^{18}F-fluoride to bone, K_i, a validated measurement of bone formation, was measured at four regions of the hip, lumbar spine, and pelvis. A significant increase in K_i was observed at all regions of interest (ROIs), including the total hip (+27%, $p = 0.002$), femoral neck (+25%, $p = 0.040$), hip trabecular ROI (+21%, $p = 0.017$), and hip cortical ROI (+51%, $p = 0.001$) in the TPT group. Significant increases in K_i in response to TPT were also observed at the lumbar spine (+18%, $p = 0.001$) and pelvis (+42%, $p = 0.001$). No significant changes in K_i were observed for the control group. Changes in BMD and bone turnover markers were consistent with previous trials of teriparatide. In conclusion, this is the first study to our knowledge to demonstrate that ^{18}F-PET can be used as an imaging biomarker for determining treatment efficacy at the hip as early as 12 weeks after initiation of therapy. © 2013 American Society for Bone and Mineral Research.

KEY WORDS: BIOMARKER; ^{18}F-FLUORIDE PET; OSTEOPOROSIS; BONE FORMATION; TREATMENT EFFICACY

Introduction

With the development of therapies for osteoporosis with novel mechanisms of action and methods of delivery, there is an increasing need for a biomarker of treatment efficacy at clinically relevant skeletal sites to accelerate drug development, particularly during early phase trials. Because of the strong relationship between bone mass and fracture risk, change in BMD is one of the principal outcomes in drug efficacy trials of bone active agents. However, changes in BMD are typically relatively small and have to be measured over many months, typically years, and this long delay between treatment initiation and the assessment of treatment efficacy is unsatisfactory. In contrast, changes in biochemical markers of bone turnover (BTMs) are both rapid and large and it has been demonstrated that early changes in BTMs predict BMD response and are significantly associated with antifracture efficacy in clinical trials of therapies for osteoporosis.[1,2] Although BTMs remain the most practical choice for measuring bone turnover, they reflect global skeletal function and cannot provide information on the effects of treatment on bone turnover at specific sites of the skeleton or differentiate treatment response at trabecular and cortical bone. This is important because while trabecular bone loss and vertebral fractures are synonymous with osteoporosis, about

Received in original form November 14, 2012; revised form December 19, 2012; accepted December 27, 2012. Accepted manuscript online January 15, 2013.
Address correspondence to: Michelle L Frost, PhD, Michelle Frost, Osteoporosis Unit, King's College London, Guy's Hospital Campus, Great Maze Pond, London, SE1 9RT, United Kingdom. E-mail: michelle.frost@kcl.ac.uk

Journal of Bone and Mineral Research, Vol. 28, No. 6, June 2013, pp 1337–1347
DOI: 10.1002/jbmr.1862

80% of all fractures occur at skeletal sites that are predominantly cortical bone.[3] Considering the critical role of cortical bone in bone strength,[4,5] the dominance of cortical over trabecular bone loss associated with increasing intracortical porosity after age 65 years,[6] and the common occurrence of nonvertebral fractures, there is a need for a new methodology to investigate treatment efficacy in cortical bone. An assessment of treatment efficacy on cortical bone at the hip is key because of the profound individual health and socioeconomic impact of hip fractures.[7]

The functional imaging technique of ^{18}F-fluoride positron emission tomography (^{18}F-PET) allows the noninvasive assessment of regional bone formation[8,9] and overcomes the important limitations of conventional techniques: It allows an assessment of regional bone formation at clinically relevant sites and, unlike bone biopsy, is noninvasive and can be readily applied in a clinical setting. The use of ^{18}F-fluoride PET for the quantitative assessment of regional bone formation was first introduced by Hawkins and colleagues in 1992.[10] After dynamic PET imaging and measurement of an arterial plasma input function, the net clearance of fluoride to the bone mineral, termed K_i, can be calculated. It has been shown that K_i correlates closely with histomorphometric parameters including the bone formation and mineral apposition rate, and therefore provides a quantitative assessment of regional bone formation.[8,9] The long-term precision of ^{18}F-PET is approximately 13%.[11] ^{18}F-PET has been used to investigate regional bone formation in patients with metabolic bone disease including those with osteoporosis and Paget's disease.[12–17] It has also been used to examine fracture healing and to assess bone viability after allogenic bone grafts and joint replacement.[18–21] The most important role of ^{18}F-PET is likely to be in clinical drug development, and a number of studies have demonstrated that it is possible to quantify the direct effects of long-term pharmacological treatments for osteoporosis and other metabolic bone diseases on bone formation rate at the spine and hip.[15,22–24]

The primary objective of this study was to determine if ^{18}F-PET can be used as an early noninvasive biomarker of treatment efficacy at the hip by examining changes in regional bone formation rate at the proximal femur in a prospective, randomized, and controlled study of postmenopausal women with osteopenia treated with the anabolic agent teriparatide for 12 weeks.

Materials and Methods

Subjects

Thirty treatment-naive postmenopausal women with a mean age of 60 years (range 51 to 71 years) with osteopenia were randomized to receive teriparatide (Forteo, Eli Lilly, Indianapolis, IN, USA) and calcium and vitamin D (TPT group, $n = 15$) or calcium and vitamin D only (control group, $n = 15$). Of these 30 subjects, 27 completed the study (13 in the TPT group and 14 in the control group). Three subjects withdrew consent after randomization and were not included in the statistical analyses. All subjects commenced calcium (1200 mg per day) and vitamin D (800 IU per day) supplements at screening and continued these for the duration of the study. Subjects in the TPT group had a short regimen (12 weeks) of treatment at the standard dose of 20 μg/day, which they commenced at baseline once all study procedures had been completed. The study consisted of three phases: a screening phase of up to 4 weeks, a treatment phase of 12 weeks, and a follow-up phase of 6 weeks during which time subjects in the TPT group discontinued teriparatide treatment. Follow-up visits were scheduled at 4, 12, 15, and 18 weeks (visit window ± 7 days) after baseline.

All subjects had a *T*-score of between −1 and −2.5 at the lumbar spine, femoral neck, and/or total hip and had osteopenia as defined by the WHO criteria.[25] None of the subjects had previously taken bisphosphonates or had any diseases known to affect bone metabolism. Seven of the subjects (4 in the control group and 3 in the teriparatide group) had taken hormone replacement therapy (HRT) previously, for on average 7.0 years (range 3 to 13 years), but all had discontinued HRT at least 12 months before enrollment. Two subjects had previously sustained a low trauma fracture, but these occurred more than 12 months before baseline. Routine laboratory tests including serum calcium, albumin-corrected calcium, alkaline phosphatase, phosphate, and parathyroid hormone were performed at screening and were within normal limits for all subjects. 25-Hydroxy vitamin D was also assessed at screening and was greater than 34 nmol/L for all subjects. Compliance with calcium and vitamin supplementation was assessed by counting the number of unused tablets at each follow-up visit. Compliance with teriparatide treatment was assessed by measuring the residual volume in the injection pens. Written informed consent was obtained from all participants, and the study was approved by the local Research Ethics Committee and UK Administration of Radioactive Substances Advisory Committee.

Measurements of BMD and biochemical markers of bone turnover

Dual-energy X-ray absorptiometry (DXA) scans were performed at the lumbar spine (L_1 to L_4), bilateral hips including femoral neck and total hip, and nondominant forearm using a Hologic Discovery (Hologic, Bedford, MA, USA) at screening (visit 1) and 18 weeks (visit 6) after baseline.

Fasting blood samples were collected at baseline and all subsequent visits for the analysis of biochemical markers of bone turnover. Samples were collected at the same time of day at each visit. Serum bone-specific alkaline phosphatase (BSAP), serum procollagen propeptide of type 1 collagen (PINP), and serum osteocalcin (OC) were measured as markers of bone formation. Serum C-terminal telopeptide (sCTX) was used as a marker of bone resorption. Bone-specific alkaline phosphatase was measured by Metra BAP immunoassay (QUIDEL); the analytical intra- and inter-run assay coefficients of variations are within 3.9% to 5.8% and 5.0% to 7.6%, respectively. PINP was measured by a two-site immunoassay based on monoclonal antibodies raised against purified intact human PINP and detecting both intact mono and trimetric forms (but not fragments) on an automated analyzer (Elecsys, Roche Diagnostics, Mannheim, Germany); the analytical intra- and interassay coefficients of variations are within 1.7% to 7.4% and 2.9% to 5.5%, respectively.

Osteocalcin was measured by two-site immunoassay recognizing both the intact and the N-terminal Mid fragment on an automatic analyzer (Elecsys); the analytical intra- and interassay coefficients of variations are within 1.3% to 6.4% and 1.8% to 3.7%, respectively. Serum CTX was measured by two-site assay using monoclonal antibodies raised against an 8 amino-acid sequence from the C-telopeptide of human type I collagen by an automatic analyzer (Elecsys); the analytical intra- and interassay coefficients of variations are within 0.0% to 9.7% and 1.4% to 6.2%, respectively. Samples were stored at −70°C and were analyzed in the same batch.

^{18}F-fluoride positron emission tomography

Full details of the acquisition and analysis of the ^{18}F-fluoride PET scans have been reported previously.[23]

Image acquisition

The PET scans were acquired on a GE Discovery PET/CT scanner (General Electric Medical Systems, Waukesha, WI, USA) with a 15.4-cm axial field of view (FOV). Subjects were positioned supine with both hips in the FOV (upper margin positioned approximately 1 cm above the acetabulum) and a low-dose computed tomography (CT) image acquired for attenuation correction and image segmentation. After an intravenous injection of 180 MBq ^{18}F-fluoride, a 60-minute dynamic scan consisting of twenty-four 5-second, four 30-second, and fourteen 240-second time frames was commenced simultaneously with the bolus injection. At the end of the dynamic scan, a single 5-minute static scan of the lumbar spine (L_1 to L_4) was acquired, starting approximately 65 minutes after the injection of tracer together with a low-dose CT scan for attenuation correction.

Image processing

The PET data were corrected for attenuation using CT data and images reconstructed by filtered back-projection using a Hanning 6.3-mm filter, resulting in 47 × 3.27-mm slices for each frame with a pixel size of 2.734 mm for PET and 0.977 mm for CT scans in the transaxial plane, respectively. The dimension and resolution of static PET and corresponding CT scans were the same as the dynamic scans.

Image analysis

The imaging scientist responsible for image analysis was blinded to both treatment arm and study visit number. All activity measurements were corrected for radioactive decay back to the time of injection. For both dynamic and static PET analysis, the bone regions of interest (ROIs) used for PET scan analysis were segmented using the CT scan images.

The dynamic PET scan images of the proximal femurs (Fig. 1*A*) were analyzed to obtain the plasma clearance to bone tissue (K_i) in four ROIs: 1) a region of mixed trabecular and cortical bone between the femoral neck and lesser trochanter anatomically equivalent to the total hip ROI used in DXA scanning (total hip ROI); 2) a region in the femoral neck with its orientation similar to that defined in DXA scanning (femoral neck ROI); 3) an elliptical fixed-size ROI (polar radius 9.81 mm) of purely trabecular bone within the trabecular section of the intertrochanteric region. The distal border of this ROI was placed one slice above the lesser trochanter with the entire ROI being outside the transverse planes intersecting the bladder (hip trabecular ROI); 4) a 60-mm-long annular cylindrical section of purely cortical bone in the femoral shaft measured from just below the lesser trochanter and excluding the medullary cavity (hip cortical ROI). There were no significant differences in K_i between the left and right hip, so results were averaged, providing a mean value for both hips. Part of the pelvis was also included within the PET scan FOV, so a ROI was placed over the whole of the pelvis included in the PET scan to obtain K_i at this skeletal site (pelvis). For the static scan analysis of the lumbar spine (Fig. 1*B*), an elliptical ROI was placed in the middle of each vertebra L_1 to L_4 excluding the end plates on the corresponding CT segmented scan (Fig. 1*C*). Each PET frame was then aligned to the corresponding CT scans. The regions were projected on the PET scans to determine the average activity concentration (kBq/mL) in each region (Fig. 1*D*). The final lumbar spine ROI was based on the average of the four individual vertebrae (lumbar spine).

The arterial plasma input function was estimated using a semipopulation curve method based on direct arterial sampling in 10 postmenopausal women.[26] Venous blood samples were collected at multiple time points during the 1-hour scan acquisition for the purpose of defining the terminal exponential for the 0- to 60-minute dynamic scan. For each subject in the present study, the population residual curve was scaled for injected activity and, after adjusting the time of peak count rate

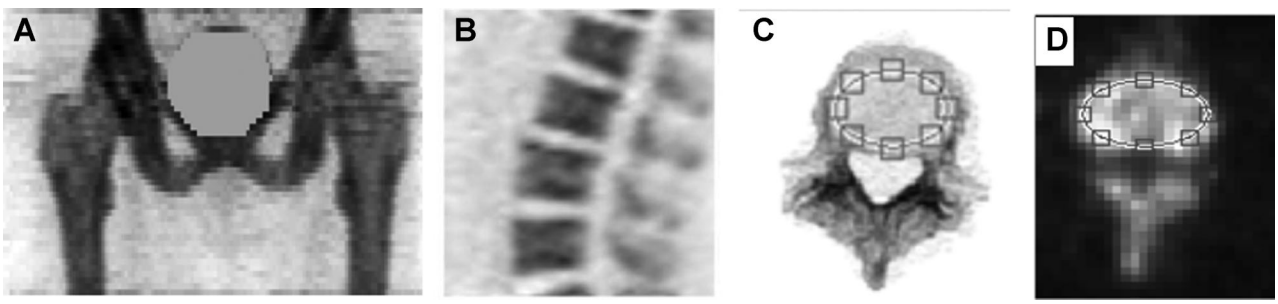

Fig. 1. ^{18}F-fluoride PET images of (*A*) proximal femur with bladder masked; (*B*) sagittal view of lumbar spine showing L_1 to L_4; (*C*) CT image of a lumbar vertebral ROI showing the elliptical lumbar spine ROI; and (*D*) lumbar spine ROI projected onto the ^{18}F-fluoride PET image.

to the time determined from an ROI drawn on the dynamic scan over the femoral artery, the scaled and time-adjusted population residual was added to the individual's terminal exponential curve to obtain the 0- to 60-minute arterial plasma input function used for kinetic analysis.[23,27]

The data from the PET dynamic scan were processed using Patlak graphical analysis to estimate regional bone plasma clearance of ^{18}F-fluoride to bone tissue (K_i) at different sites at the hip and pelvis. The Patlak plot, described in full elsewhere,[12,19,28] is a graphical analysis technique that assumes that $^{18}F^-$ is taken up by two compartments, a central compartment that is in rapid equilibrium with plasma and a peripheral bone mineral compartment that tracer enters without ever leaving during the time of the measurements. The net amount of tracer in the bone ROI is given by:

$$C_{tissue}(T) = K_i \int_0^T C_{plasma}(t)dt + V_0\, C_{plasma}(T) \quad (1)$$

where t is time, $C_{tissue}(T)$ is the total amount of tracer in the bone ROI at time T after injection, $C_{plasma}(T)$ is the concentration of tracer in plasma, K_i is the plasma clearance describing the rate of entry into the peripheral compartment, and V_0 is the volume of distribution of tracer in the central compartment. To allow for equilibration between tracer in plasma and the central compartment, the value of K_i was determined by fitting the dynamic scan data from 10 to 60 minutes after injection.

A novel and validated method for estimating K_i using static scan data only was used to estimate K_i at the lumbar spine, described in detail previously.[29] K_i is estimated using the value of $C_{tissue}(T)$ in equation 1 obtained from a single static frame. A value of $V_0 = 0.44$ for the lumbar spine regions was used based on the mean value obtained for a previous study.[29] A measurement of *Ki* rather than the calculation of standardized uptake value (SUV), the most widely used index in PET oncology, is preferable because we have previously shown that changes in SUV do not necessarily reflect the true changes in metabolic activity at the measurement site, particularly with potent bone active agents such as TPT.[23]

The bone plasma clearance of ^{18}F-fluoride to bone tissue, K_i, has been shown to be highly correlated with indices of bone formation, including the bone formation and mineral apposition rate, and therefore provides a quantitative assessment of regional bone formation.[8,9]

Statistical analysis

Baseline characteristics were expressed as the mean and standard deviation (SD) and compared using Student's t test. Each variable was tested for normality and parametric and nonparametric tests applied accordingly. Absolute values and percentage change from baseline in BMD and the ^{18}F-PET parameter K_i were expressed as the mean and SD. The reported percentage changes reflect the mean percentage change for individual subjects rather than the percent difference in the mean absolute values at baseline and 12 weeks (because of the variations in baseline values, the latter is typically lower than the former). Changes in BMD and K_i from baseline were evaluated using a paired t test. Differences in changes from baseline in BMD and K_i between the TPT and control groups were evaluated using an unpaired t test. Absolute values and percentage changes from baseline in BTMs were expressed as the median and interquartile range. Changes in BTMs from baseline were evaluated using a Wilcoxon signed rank test. Differences in changes from baseline in BTMs between the TPT and control groups were evaluated using a Mann-Whitney U test. Correlations between changes in K_i and changes in BTMs at 12 weeks follow-up for the TPT group only were assessed using the Spearman rank correlation test. A p value of 0.05 or less was considered statistically significant.

To determine sample size, a difference of 22% in K_i at the hip (primary outcome) was assumed between the TPT and control groups at 12 weeks and a standard deviation of 13%.[11] A total of 15 subjects in each group would provide more than 90% power to detect a significance difference between groups with a type 1 error of $p = 0.05$.

Results

Study population

Baseline characteristics are shown in Table 1. All women were postmenopausal with a mean time since menopause of 11.7 and 11.4 years for the TPT and control groups, respectively. All subjects were classified as osteopenic at the spine and/or hip with a mean lumbar spine T-score of –1.7 and –1.4 for the TPT and control groups, respectively. Serum chemistry results were within normal limits for all subjects. There were no significant differences in any of the baseline characteristics between the two study groups. One subject in the TPT group discontinued her calcium and vitamin D supplements 4 weeks after her baseline visit and did not recommence these for the remainder of the study. Compliance with calcium and vitamin D supplements averaged 98% (range 89% to 100%) for both study groups

Table 1. Baseline Study Group Characteristics[a]

Variable	Teriparatide	Control
n	13	14
Age (years)	59.6 (4.8)	60.1 (4.6)
Years postmenopausal	11.7 (4.8)	11.4 (6.3)
Height (cm)	161.2 (7.8)	162.8 (5.3)
Weight (kg)	65.1 (8.2)	64.3 (9.0)
BMI (kg/m^2)	25.1 (2.7)	24.2 (2.8)
Lumbar spine BMD T-score	−1.68 (0.62)	−1.36 (1.02)
Mean femoral neck BMD T-score	−1.45 (0.59)	−1.30 (0.78)
Mean total hip BMD T-score	−0.97 (0.48)	−0.84 (0.57)
Ultradistal forearm BMD T-score	−1.33 (1.2)	−0.88 (0.71)
Serum calcium (mmol/L)	2.32 (0.07)	2.32 (0.05)
Serum albumin-corrected calcium (mmol/L)	2.32 (0.07)	2.30 (0.06)
Serum phosphate (mmol/L)	1.17 (0.11)	1.21 (0.14)
Serum alkaline phosphatase (IU/L)	69.38 (22.01)	73.14 (26.29)
Parathyroid hormone (ng/L)	38.31 (14.72)	44.64 (11.18)
25-hydroxy vitamin D (nmol/L)	77.00 (30.74)	63.71 (22.25)

BMI = body mass index; BMD = bone mineral density.
[a]Data are means (SD).

(excluding the subject who discontinued supplements). Teriparatide treatment was well tolerated by all subjects and treatment compliance averaged 89.7%. No serious adverse events occurred during the study.

Bone density measurements and biochemical markers of bone turnover

The follow-up BMD scans were performed 18 weeks after the baseline visit and 6 weeks after the subjects in the TPT group discontinued treatment. The mean percentage changes in BMD at the lumbar spine, femoral neck, total hip, and ultradistal forearm are shown in Table 2. There was a significant increase in BMD at the lumbar spine and total hip in the TPT group, averaging 2.6% and 0.9%, respectively, at 18 weeks. There were no significant changes in BMD for either group at the femoral neck or nondominant forearm.

After 12 weeks of teriparatide treatment, there were highly statistically significant increases in PINP, OC, and sCTX in the TPT group of +86%, +92%, and +54%, respectively. Modest but statistically significant decreases in PINP, BSAP, and OC were observed in the control group. The changes in BTMs were significantly greater for the TPT group compared with the control group (Table 2, Fig. 2). After discontinuation of treatment at 12 weeks in the TPT group, levels of PINP, osteocalcin, and sCTX decreased at 15 and 18 weeks but remained statistically higher than baseline values at 18 weeks (Fig. 2).

Quantitative measurements of bone formation using ^{18}F-fluoride PET

Mean plasma clearance of ^{18}F-fluoride to bone, K_i, at baseline and 12 weeks and the percentage change for both the TPT and control groups are shown in Table 2 and Fig. 3. A significant increase in K_i was observed at all sites at the hip including the total hip (+27%, $p = 0.002$), femoral neck (+25%, $p = 0.04$), hip trabecular ROI (+21%, $p = 0.017$), and hip cortical ROI (+51%, $p = 0.001$) in the TPT group. Baseline values of K_i at the lumbar spine were on average twice that observed at the hip regions for both study groups. Mean results at baseline for the pelvis were similar to those observed at the femoral neck. Significant increases in K_i in response to TPT were also observed at the lumbar spine (+18%, $p = 0.001$) and pelvis (+42%, $p = 0.001$) (Table 2, Fig. 3). No significant changes in K_i were observed for the control group at any of the hip ROIs or at the pelvis or lumbar spine. The changes observed for the TPT group were significantly greater than those observed for the control group for all sites with the exception of the femoral neck and hip trabecular ROI (Table 2, final column).

The individual changes observed for the 13 subjects randomized to receive teriparatide at the hip regions, pelvis, and lumbar spine are shown in Fig. 4. K_i increased in 11 of 13 subjects at the hip ROIs. Two subjects showed decreases in K_i at the total hip, femoral neck, and hip cortical ROI (Fig. 4*A, B, D*). K_i at the hip trabecular ROI and pelvis also decreased for one of these subjects (Fig. 4*C, E*). K_i increased at the lumbar spine in all subjects in the TPT group (Fig. 4*F*).

There was a significant correlation between changes in K_i at the hip cortical ROI and both PINP ($r = 0.70$, $p = 0.008$) and BSAP ($r = 0.56$, $p = 0.046$). No other significant correlations were observed between changes in K_i and changes in BTMs.

Discussion

The purpose of this study was to investigate the role of ^{18}F-PET as an imaging biomarker of treatment efficacy at the clinically important skeletal site of the hip. This is of particular interest because of the recent acceleration of drugs being approved for the treatment of osteoporosis. This study demonstrated that the anabolic agent TPT is having a profound effect on bone as early as 12 weeks from the initiation of therapy with highly significant increases in regional bone formation, measured using ^{18}F-PET, at the hip, pelvis, and lumbar spine (Table 2, Fig. 3). Differences in the magnitude of these increases were seen for different regions within the hip and between the hip and both the pelvis and lumbar spine, demonstrating significant heterogeneity in response to treatment at different sites of the skeleton (Fig. 3). Results from this study contribute significantly toward the validation of the use of ^{18}F-PET as a noninvasive imaging biomarker of treatment efficacy at multiple sites of the skeleton.

In agreement with a previous single-arm study of postmenopausal women with osteoporosis treated with TPT for 6 months by the same authors,[23] percentage changes in K_i were greatest at the hip (Table 2, Fig. 3). In a study by Moore and colleagues using ^{99m}Tc-MDP bone scans to examine regional changes in bone in response to teriparatide, greater increases in ^{99m}Tc-MDP plasma clearance at the skull were observed compared with the spine, and greatest visual increases in tracer uptake at the skull and lower extremities on whole body bone scans.[30] K_i increased at all hip sites in response to 12 weeks of teriparatide treatment, ranging from 21% at the hip trabecular ROI to 51% for the hip cortical ROI. K_i also increased at the pelvis (+42.1%, $p = 0.001$) and lumbar spine (+17.8%, $p = 0.001$) (Table 2). An animal study by Sato and colleagues of the effects of TPT on the proximal femur also reported an increase in bone formation rate of 84%, measured at the femoral neck cortex using conventional bone histomorphometry, supporting the results obtained in the present study showing that bone formation does increase significantly in response to TPT at this skeletal site.[31] The reason for a larger response, in terms of increase in *Ki*, in cortical regions within the hip compared with those observed at other ROIs of the hip, with a larger trabecular component, and at the purely trabecular ROI within the lumbar vertebral body, may in part be explained by the increase in intracortical and endocortical bone surfaces seen after menopause and with aging.[6,32] In a sophisticated study by Zebaze and colleagues using hrQCT, both intracortical porosity and trabeculization of the cortex increased with age, increasing the amount of intracortical surface exposed, on which remodeling occurs.[6] Further data obtained using postmortem femur specimens showed that in older women the intracortical surface was larger than the trabecular surface in the subtrochanteric region.[6] Because TPT stimulates bone formation through modeling, by direct apposition on endosteal and periosteal surfaces and through endocortical and intracortical remodeling, the availability of a large remodeling surface within cortical bone along with the endocortical surface will increase

Table 2. ^{18}F-fluoride PET Parameters, Biochemical Markers, and BMD at Baseline and Follow-up for the Teriparatide and Control Groups

	Teriparatide group ($n = 13$)				Control group ($n = 14$)				
^{18}F-fluoride PET K_i[a]	Baseline	12 weeks	% Change	p Value[b]	Baseline	12 weeks	% Change	p Value[b]	p Value[c]
Total hip (mL min^{-1} mL^{-1})	0.012 (0.003)	0.014 (0.004)	+26.5 (26.4)	0.002	0.012 (0.003)	0.012 (0.003)	+2.8 (20.9)	0.866	0.015
Femoral neck (mL min^{-1} mL)[d]	0.013 (0.004)	0.015 (0.005)	+25.2 (37.6)	0.040	0.014 (0.003)	0.014 (0.003)	+5.5 (26.6)	0.776	0.137
Hip trabecular ROI (mL min^{-1} mL^{-1})	0.013 (0.003)	0.015 (0.004)	+20.5 (25.4)	0.017	0.014 (0.004)	0.015 (0.004)	+9.1 (25.2)	0.309	0.255
Hip cortical ROI (mL min^{-1} mL^{-1})	0.009 (0.002)	0.013 (0.003)	+50.7 (42.6)	0.001	0.009 (0.002)	0.010 (0.003)	+8.0 (27.7)	0.422	0.005
Pelvis (mL min^{-1} mL^{-1})	0.013 (0.003)	0.018 (0.005)	+42.1 (35.8)	0.001	0.013 (0.003)	0.015 (0.004)	+10.9 (29.9)	0.294	0.021
Lumbar spine (mL min^{-1} mL^{-1})	0.024 (0.004)	0.028 (0.005)	+17.8 (10.1)	0.001	0.027 (0.004)	0.028 (0.003)	+5.7 (16.9)	0.306	0.040
Biochemical markers[e]	Baseline	12 weeks	% Change	p Value[f]	Baseline	12 weeks	% Change	p Value[f]	p Value[g]
PINP (ng/mL)	49.3 (16.7)	86.2 (91.2)	+85.9 (104.9)	0.001	60.9 (29.0)	46.9 (25.0)	−20.3 (16.9)	0.002	<0.001
BSAP (mU/mL)	24.4 (10.9)	25.9 (17.8)	+9.3 (37.0)	0.116	25.3 (13.3)	25.1 (9.95)	−8.0 (17.6)	0.016	0.008
Osteocalcin (ng/mL)	24.3 (11.9)	44.5 (24.6)	+91.8 (61.6)	0.001	26.7 (10.4)	22.1 (9.1)	−14.0 (16.8)	0.010	<0.001
sCTX (ng/mL)	0.34 (0.33)	0.56 (0.52)	+53.6 (77.3)	0.011	0.48 (0.30)	0.48 (0.26)	+1.5 (27.5)	0.638	0.009
DXA bone mineral density[a]	Baseline	18 weeks	% Change	p Value[b]	Baseline	18 weeks	% Change	p Value[b]	p Value[c]
Lumbar spine (BMD g/cm^2)	0.86 (0.07)	0.88 (0.06)	+2.6 (3.2)	0.012	0.90 (0.11)	0.89 (0.12)	−0.5 (2.3)	0.505	0.009
Femoral neck (BMD g/cm^2)	0.69 (0.06)	0.69 (0.06)	+0.8 (1.7)	0.139	0.71 (0.09)	0.71 (0.10)	+0.3 (2.0)	0.437	0.550
Total hip (BMD g/cm^2)	0.82 (0.06)	0.83 (0.06)	+0.9 (1.1)	0.012	0.84 (0.07)	0.84 (0.08)	+0.1 (1.7)	0.722	0.205
Ultradistal forearm (BMD g/cm^2)	0.36 (0.10)	0.36 (0.09)	+0.2 (2.4)	0.972	0.39 (0.08)	0.38 (0.08)	−0.6 (2.2)	0.256	0.711

PET = positron emission tomography; BMD = bone mineral density; ROI = region of interest; PINP = procollagen propeptide of type 1 collagen; BSAP = bone-specific alkaline phosphatase; sCTX = C-terminal telopeptide; DXA = dual-energy X-ray absorptiometry.

[a]Absolute values at baseline and follow-up are mean and SD. Results for percent change from baseline are mean and SD for individual subjects.

[b]12 weeks versus baseline calculated using paired t test.

[c]Mean percent change for teriparatide versus control groups calculated using unpaired t test.

[d]Unable to obtain valid result for 1 subject in the control group at 12 weeks.

[e]Absolute values at baseline and follow-up are median and interquartile range. Results for percent change from baseline are median and interquartile range for individual subjects.

[f]18 weeks versus baseline calculated using Wilcoxon signed rank test.

[g]Median percent change for teriparatide versus control groups calculated using Mann-Whitney U test.

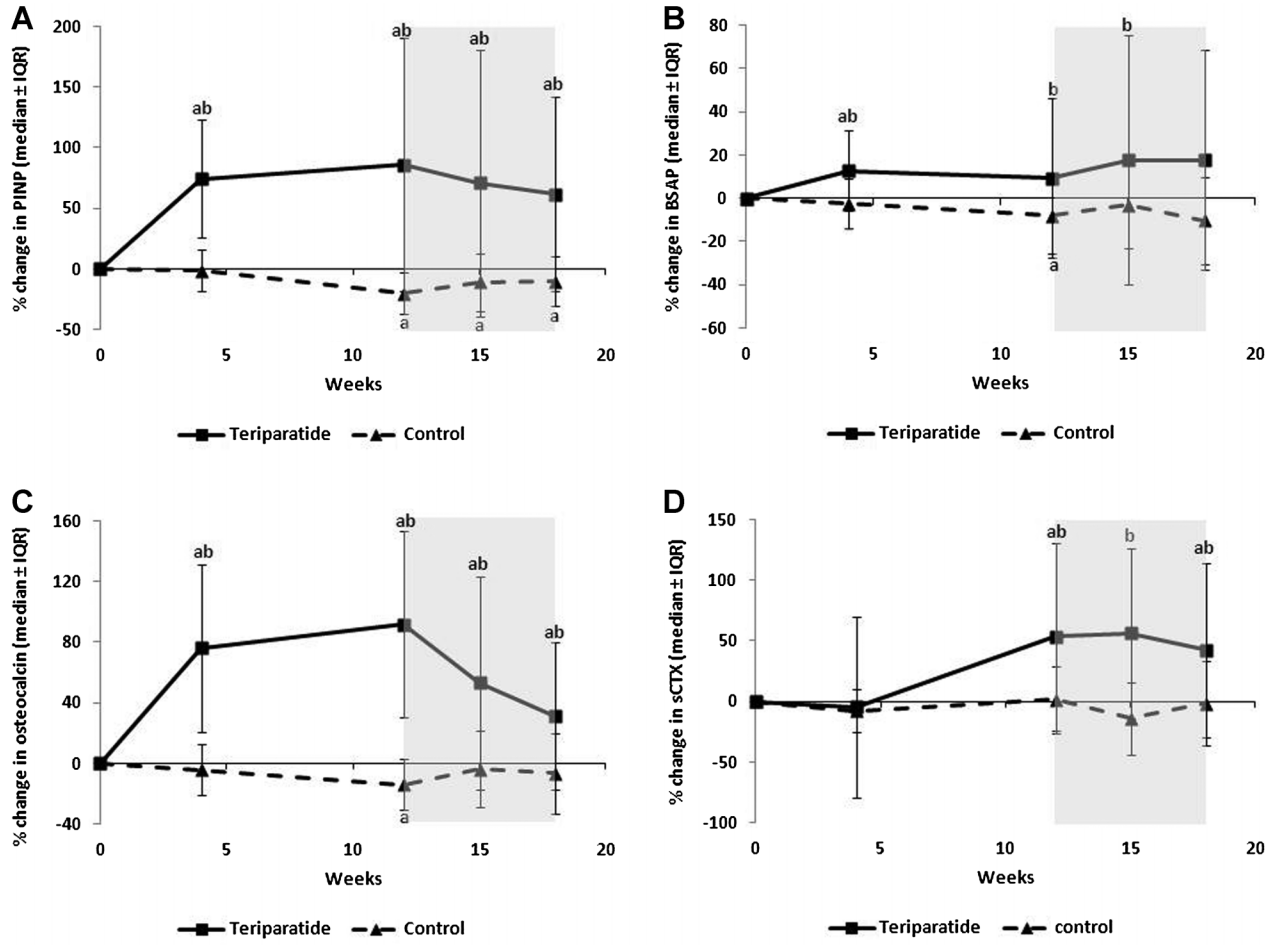

Fig. 2. Median percent changes from baseline in bone turnover markers measured at 4, 12, 15, and 18 weeks. Subjects in the TPT droup discontinued daily TPT treatment at 12 weeks and did not receive any further treatment for the remainder of the study (shaded area). [a]$p < 0.05$ versus baseline using the two-sided Wilcoxon signed rank test. [b]$p < 0.05$ TPT median % changes versus the control group calculated using the Mann-Whitney *U* test. (*A*) Serum procollagen propeptide of type I collagen (PINP); (*B*) bone-specific alkaline phosphatase (BSAP); (*C*) osteocalcin (OC); (*D*) serum C-telopeptide of type I collagen (sCTX).

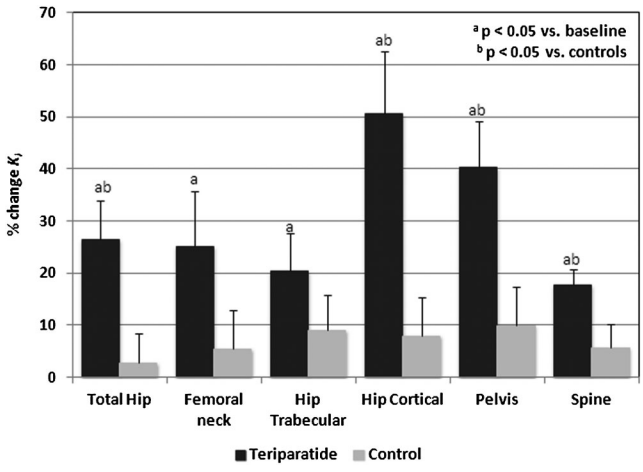

Fig. 3. Mean percent change in regional bone formation (K_i) at the hip, pelvis, and lumbar spine at 12 weeks. [a]$p < 0.05$ at 12 weeks versus baseline calculated using the paired *t* test. [b]$p < 0.05$ TPT versus control group using unpaired *t* test.

bone formation rate at sites of predominantly cortical bone. The increase in K_i observed at the pelvis was also large (+42.1%) and was greater than that observed at the total hip and femoral neck (Table 2). This was unexpected, given the high proportion of trabecular bone in the pelvis and in view of the general observation of higher increases in K_i at sites of predominantly cortical rather than trabecular bone. This could reflect the small sample size because this study was not powered to detect significant differences between skeletal sites in changes in K_i. However, it could also reflect differences in anatomical structure between the pelvis and proximal femur, the fact that the pelvis consists of primarily low-density trabecular bone, and variations in loading at the pelvis with load-induced stresses being up to 50 times higher in the cortical shell than in the underlying trabecular bone.[33] The latter, combined with the known synergistic effect of TPT treatment with loading,[34] could indicate much of the increase in K_i at the pelvis is occurring in cortical bone, although it is not possible to validate this because of the limited spatial resolution of PET.

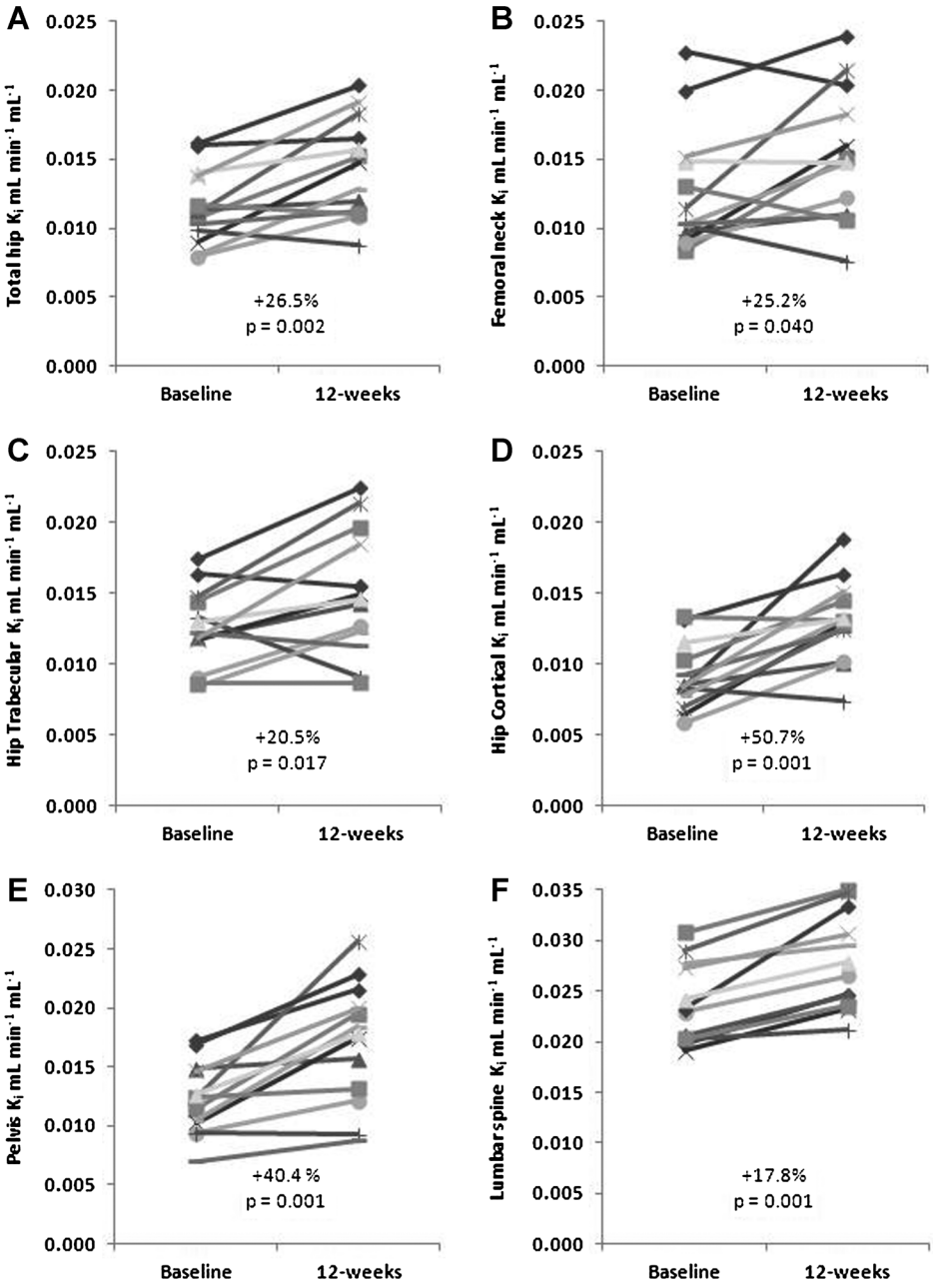

Fig. 4. Plots of the baseline to 12-week changes in K_i for the 13 individual subjects in the TPT group at the (*A*) total hip; (*B*) femoral neck; (*C*) hip trabecular ROI; (*D*) hip cortical ROI; (*E*) pelvis; and (*F*) lumbar spine. The *p* values represent statistical significance of mean percent change from baseline calculated using the paired *t* test.

A significant but modest increase in BMD was observed at the lumbar spine (+2.6%, $p = 0.012$) and total hip (+0.9%, $p = 0.012$) in response to TPT (Table 2). The early timing of the DXA scan limits any useful comparison with other studies, but results from the pivotal fracture trials of TPT showed that changes in areal BMD are greatest at the lumbar spine, with only relatively modest gains or even loss in BMD being seen at the hip.[35–38] As observed in an earlier 6-month study of the effect of TPT treatment at the lumbar spine,[23] there was a disparity between the changes in regional bone formation and results from studies of the effects of teriparatide on BMD at the spine and hip.[35–39] The increases in BMD at the hip are relatively modest compared with those observed at the lumbar spine.[35–39] These results show that large changes in K_i, ie, an increase in bone formation at the hip, do not necessarily translate into increases in bone density, at least with TPT. The early net increase in K_i at the spine is accompanied by a significant increase in lumbar spine BMD (Table 2). This increase in BMD at the lumbar spine is consistent with previous clinical trials of TPT.[39,40] The large early gains in lumbar spine BMD in response to TPT has not been observed at the hip or forearm, with evidence of a small decline in BMD during the first 6 months of TPT or PTH 1–84 treatment.[35,40,41] The diminished or lack of a response of BMD at the hip and other long bones[42] is thought to be a consequence of the transient

increase in cortical porosity that accompanies the increased rate of remodeling with TPT.[31,43] This reduction in BMD is compensated by direct endocortical and periosteal apposition[42,44] and increased trabecular bone volume.[45] These competing factors of periosteal and endocortical apposition, transient bone loss through intracortical bone remodeling and increased trabecular bone volume, combined with any change in hip BMD being confounded by changes in geometry,[44] results in no change, a slight increase, or even a loss in hip BMD during early treatment. This highlights the limitations of relying on bone densitometric techniques alone, such as DXA or quantitative CT, as a surrogate determinant of treatment efficacy, particularly at sites of predominantly cortical bone and with anabolic agents, such as TPT, which increase remodeling activity.

The early changes in K_i are consistent with the early changes observed with BTMs in the large trials of TPT,[35,37] demonstrating the early rapid and large rise in bone formation markers within the first month of treatment and increases in bone resorption occurring later at approximately 3 months, as observed in the current study (Fig. 2). The rapid treatment offset effect found in larger trials of TPT[46] was also observed with markers of bone formation decreasing at 15 and 18 weeks after treatment discontinuation at 12 weeks (Fig. 2). When the changes in BTMs and K_i were compared, a significant correlation was only observed between changes in K_i at the hip cortical ROI (TPT group only) and changes in PINP ($r = 0.70$, $p = 0.008$) and BSAP ($r = 0.56$, $p = 0.046$). The lack of a correlation between K_i at other ROIs and BTMs is likely owing to the small sample size and the fact that changes in BTMs reflect changes for the entire skeleton and are likely to underestimate treatment response at skeletal sites, which show large changes in response to a pharmacological intervention. This further supports the use of ^{18}F-PET because it can be used to differentiate between the responses in trabecular and cortical bone.

For ^{18}F-PET to be used as a biomarker tool for the evaluation of novel drugs, it must be demonstrated that K_i changes in response to osteoporosis therapy in a predictable way according to the known mechanism of action of the therapy.[1] Previous studies have reported significant reductions in K_i at the lumbar spine in postmenopausal women with low BMD treated with the antiresorptive risedronate[22] and at the lumbar spine and femoral neck in patients with glucocorticoid-induced osteoporosis treated with alendronate.[24] Increases in K_i in response to the anabolic treatment TPT have been observed in the current randomized, controlled 12-week study and an earlier single-arm study of the long-term (6 months) effect of TPT treatment at the lumbar spine.[23] It must also be demonstrated that the measurement parameter K_i is measuring a clinically relevant biological process and that measurement precision is acceptable. ^{18}F-fluoride PET has been validated by direct comparison with bone biopsy in one animal study[9] and one clinical study.[8] Although small, results from these studies showed that K_i was highly correlated with histomorphometric indices of bone formation and mineral apposition rate,[8,9] which is consistent with the known mechanism of uptake of fluoride ions in newly forming hydroxyapatite crystals.[47] A study by the same authors showed that the long-term precision of ^{18}F-PET is approximately 13%.[11] The large changes in K_i observed in response to treatment combined with a long-term coefficient of variation (CV) of 13% means that treatment efficacy can be assessed in a relatively small number of subjects, making ^{18}F-PET especially suitable for pilot studies or an imaging substudy in larger trials with BMD or fracture as the primary outcome. Furthermore, unlike other imaging biomarkers in osteoporosis such as BMD by DXA or QCT and trabecular microarchitecture measurements by MRI or high-resolution pQCT, changes in response to therapy can be measured within weeks rather than months or years.

In conclusion, this study demonstrates that ^{18}F-PET can be used as an imaging biomarker for determining treatment efficacy at the hip and other skeletal sites, and at least for anabolic agents, response to treatment can be assessed as early as 12 weeks after initiation of therapy. ^{18}F-PET offers important advantages over conventional techniques including being noninvasive and providing information on the effects of treatment at clinically important skeletal sites. The precision of ^{18}F-PET is comparable to that found for biochemical markers of global bone metabolism, and this, combined with the large changes observed in response to an anabolic agent, means that treatment efficacy can be determined in a small number of subjects. The measurement of treatment efficacy at the hip is especially important because the loss of cortical bone in the pathophysiology of osteoporosis-related fractures, particularly after the age of 60 years, is increasingly being recognized. This shift of focus from trabecular to cortical bone is also likely to change treatment decision making, with different therapeutic interventions being targeted according to the age of the patient, and will also lead to the acceleration of the development of bone-active agents that target cortical bone specifically.

Disclosures

MF, GMB, and IF received a research grant from Novartis Pharma to perform this study. DL, BB, US, M-AV, and TD are employees of Novartis Pharma and hold stock options in Novartis. IF is a member of an advisory board for Servier. AEM, MS, PKM, and PJS state that they have no conflicts of interest.

Acknowledgments

This work was supported by Novartis Pharma.

Authors' roles: Study design: MLF, GMB, DL, US, TP, and IF. Study conduct: MLF, AEM, GMB, IF, PKM, and PJS. Data collection: MLF, AEM, and IF. Data analysis: MLF, MS, GMB, and MV. Data interpretation: MLF, MS, GMB, DL, BB, US, MV, and IF. Drafting manuscript: MLF. Revising manuscript content: GMB, DL, BB, US, MV, TP, PKM, PJS, and IF. Approving final version of manuscript: all authors. MLF, GMB, and IF take responsibility for the integrity of the data analysis.

References

1. Bouxsein ML, Delmas PD. Considerations for development of surrogate endpoints for antifracture efficacy of new treatments in osteoporosis: a perspective. J Bone Miner Res. 2008;23(8):1155–67.
2. Leeming DJ, Alexandersen P, Karsdal MA, Qvist P, Schaller S, Tankó LB. An update on biomarkers of bone turnover and their utility in

biomedical research and clinical practice. Eur J Clin Pharmacol. 2006;62:781–92.

3. Kanis JA, Johnell O, Oden A, Dawson A, De Laet C, Jonsson B. Ten year probabilities of osteoporotic fractures according to BMD and diagnostic thresholds. Osteoporos Int. 2001;12:989–95.
4. Burr DB. Cortical bone: a target for fracture prevention?. Lancet. 2010;375:1672–3.
5. Holzer G, von Skrbensky G, Holzer LA, Pichl W. Hip fractures and the contribution of cortical versus trabecular bone to femoral neck strength. J Bone Miner Res. 2009;24:468–74.
6. Zebaze RM, Ghasem-Zadeh A, Bohte A, Iuliano-Burns S, Mirams M, Price RI, Mackie EJ, Seeman E. Intracortical remodelling and porosity in the distal radius and post-mortem femurs of women: a cross-sectional study. Lancet. 2010;375:1729–36.
7. Hartholt KA, Oudshoorn C, Zielinski SM, Burgers PT, Panneman MJ, van Beeck EF, Patka P, van der Cammen TJ. The epidemic of hip fractures: are we on the right track?. PLoS One. 2011;6:e22227.
8. Messa C, Goodman WG, Hoh CK, Choi Y, Nissenson AR, Salusky IB, Phelps ME, Hawkins RA. Bone metabolic activity measured with positron emission tomography and ^{18}F-fluoride ion in renal osteodystrophy: correlation with bone histomorphometry. J Clin Endo Metab. 1993;77:949–55.
9. Piert M, Zittel TT, Becker GA, Jahn M, Stahlschmidt A, Maier G, Machulla HJ, Bares R. Assessment of porcine bone metabolism by dynamic ^{18}F-fluoride PET: correlation with bone histomorphometry. J Nucl Med. 2001;42:1091–100.
10. Hawkins RA, Choi Y, Huang S-C, Hoh CK, Dahlbom M, Schiepers C, Satyamurthy N, Barrio JR, Phelps ME. Evaluation of the skeletal kinetics of fluorine-18-fluoride ion with PET. J Nucl Med. 1992;33: 633–42.
11. Siddique M, Frost ML, Blake GM, Moore AE, Al-Beyatti Y, Marsden PK, Schleyer PJ, Fogelman I. The precision and sensitivity of ^{18}F-fluoride PET for measuring regional bone metabolism: a comparison of quantification methods. J Nucl Med. 2011;52:1748–55.
12. Cook GJR, Blake GM, Marsden PK, Cronin B, Fogelman I. Quantification of skeletal kinetic indices in Paget's disease using dynamic ^{18}F-fluoride positron emission tomography. J Bone Miner Res. 2002;17:854–9.
13. Frost ML, Fogelman I, Blake GM, Marsden PK, Fogelman I. Dissociation between global markers of bone formation and direct measurement of spinal bone formation in osteoporosis. J Bone Miner Res. 2004;19:1797–804.
14. Frost ML, Blake GM, Cook GJ, Marsden PK, Fogelman I. Differences in regional bone perfusion and turnover between lumbar spine and distal humerus: ^{18}F-fluoride PET study of treatment-naïve and treated postmenopausal women. Bone. 2009;45:942–8.
15. Installe J, Nzeusseu A, Bol A, Depresseux G, Devogelaer JP, Lonneux M. ^{18}F-fluoride PET for monitoring therapeutic response in Paget's disease of bone. J Nucl Med. 2005;46:1650–8.
16. Piert M, Zittel TT, Jahn M, Stahlschmidt A, Becker GA, Machulla H-J. Increased sensitivity in detection of a porcine high-turnover osteopenia after total gastrectomy by dynamic ^{18}F-fluoride ion PET and quantitative CT. J Nucl Med. 2003;44:117–24.
17. Schiepers C, Nuyts J, Bormans G, Dequeker J, Bouillon R, Mortelmans L, Verbruggen A, De Roo M. Fluoride kinetics of the axial skeleton measured in vivo with fluorine-18-fluoride PET. J Nucl Med. 1997; 38:1970–6.
18. Berding G, Burchert W, van den Hoff J, Pytlik C, Neukam FW, Meyer GJ, Gratz KF, Hundeshagen H. Evaluation of the incorporation of bone grafts used in maxillofacial surgery with ^{18}F-fluoride ion and dynamic positron emission tomography. Eur J Nucl Med. 1995;22:1133–40.
19. Brenner W, Vernon C, Muzi M, Mankoff DA, Link JM, Conrad EU, Eary JF. Comparison of different quantitative approaches to ^{18}F-fluoride PET scans. J Nucl Med. 2004;45:1493–500.
20. Hsu WK, Feeley BT, Krenek L, Stout DB, Chatziioannou AF, Lieberman JR. The use of ^{18}F-fluoride and ^{18}F-FDG PET scans to assess fracture healing in a rat femur model. Eur J Nucl Med Mol Imaging. 2007;34:1291–301.
21. Piert M, Winter E, Becker GA, Bilger K, Machulla H, Müller-Schauenburg W, Bares R, Becker HD. Allogenic bone graft viability after hip revision arthroplasty assessed by dynamic ^{18}F-fluoride ion positron emission tomography. Eur J Nucl Med. 1999;26:615–24.
22. Frost ML, Cook GJ, Blake GM, Marsden PK, Benatar NA, Fogelman I. A prospective study of risedronate on regional bone metabolism and blood flow at the lumbar spine measured by ^{18}F-fluoride positron emission tomography. J Bone Miner Res. 2003;18:2215–22.
23. Frost ML, Siddique M, Blake GM, Moore AE, Schleyer PJ, Dunn JT, Somer EJ, Marsden PK, Eastell R, Fogelman I. Differential effects of teriparatide on regional bone formation using ^{18}F-fluoride positron emission tomography. J Bone Miner Res. 2011;26:1002–11.
24. Uchida K, Nakajima H, Miyazaki T, Yayama T, Kawahara H, Kobayashi S, Tsuchida T, Okazawa H, Fujibayashi Y, Baba H. Effects of alendronate on bone metabolism in glucocorticoid-induced osteoporosis measured by ^{18}F-fluoride PET: a prospective study. J Nucl Med. 2009;50:1808–14.
25. World Health Organization. Assessment of fracture risk and its application to screening for postmenopausal osteoporosis. Technical Support Series, No 843 Geneva, Switzerland: WHO, 1994.
26. Cook GJR, Lodge MA, Marsden PK, Dynes A, Fogelman I. Non-invasive assessment of skeletal kinetics using fluorine-18-fluoride positron emission tomography: evaluation of image and population-derived arterial input functions. Eur J Nuc Med. 1999;26:1424–9.
27. Blake GM, Siddique M, Puri T, Frost ML, Moore AE, Cook GJ, Fogelman I. A semipopulation input function for quantifying static and dynamic ^{18}F-fluoride PET scans. Nucl Med Commun. 2012;33:881–8.
28. Patlak CS, Blasberg RG, Fenstermacher JD. Graphical evaluation of blood-to-brain transfer constants from multiple-time uptake data. J Cereb Blood Flow Metab. 1983; 3: 1–7.
29. Siddique M, Blake GM, Frost ML, Moore AE, Puri T, Marsden PK, Fogelman I. Estimation of regional bone metabolism from whole-body ^{18}F-Fluoride PET Static Images. Eur J Nuc Med Mol Imaging. 2012;39:337–43.
30. Moore AE, Blake GM, Taylor KA, Rana AE, Wong M, Chen P, Fogelman I. Assessment of regional changes in skeletal metabolism following 3 and 18 months of teriparatide treatment. J Bone Miner Res. 2010;25:960–7.
31. Sato M, Westmore M, Ma YL, Schmidt A, Zeng QQ, Glass EV, Vahle J, Brommage R, Jerome CP, Turner CH. Teriparatide [PTH(1–34)] strengthens the proximal femur of ovariectomized nonhuman primates despite increasing porosity. J Bone Miner Res. 2004;19:623–9.
32. Bjørnerem Å, Ghasem-Zadeh A, Bui M, Wang X, Rantzau C, Nguyen TV, Hopper JL, Zebaze R, Seeman E. Remodeling markers are associated with larger intracortical surface area but smaller trabecular surface area: a twin study. Bone. 2011;49:1125–30.
33. Dalstra M, Huiskes R. Load transfer across the pelvic bone. J Biomechanics. 1995;28:715–24.
34. Hagino H, Okano T, Akhter MP, Enokida M, Teshima R. Effect of parathyroid hormone on cortical bone response to in vivo external loading of the rat tibia. J Bone Miner Metab. 2001;19:244–50.
35. Black DM, Greenspan SL, Ensrud KE, Palermo L, McGowan JA, Lang TF, Garnero P, Bouxsein ML, Bilezikian JP, Rosen CJ. PaTH Study Investigators. The effects of parathyroid hormone and alendronate alone or in combination in postmenopausal osteoporosis. N Engl J Med. 2003;349:1207–15.
36. Borggrefe J, Graeff C, Nickelsen TN, Marin F, Glüer CC. Quantitative computed tomographic assessment of the effects of 24 months of teriparatide treatment on 3D femoral neck bone distribution, geometry, and bone strength: results from the EUROFORS study. J Bone Miner Res. 2010;25:472–81.

37. Lindsay R, Nieves J, Formica C, Henneman E, Woelfert L, Shen V, Dempster D, Cosman F. Randomised controlled study of effect of parathyroid hormone on vertebral-bone mass and fracture incidence among postmenopausal women on oestrogen with osteoporosis. Lancet. 1997;350:550–5.

38. Neer RM, Arnaud CD, Zanchetta JR, Prince R, Gaich GA, Reginster JY, Hodsman AB, Eriksen EF, Ish-Shalom S, Genant HK, Wang O, Mitlak BH. Effect of recombinant human parathyroid hormone (1–34) fragment on spine and non-spine fractures and bone mineral density in postmenopausal osteoporosis. N Engl J Med. 2001;344:1434–41.

39. Bauer DC, Garnero P, Bilezikian JP, Greenspan SL, Ensrud KE, Rosen CJ, Palermo L, Black DM. Short-term changes in bone turnover markers and bone mineral density response to parathyroid hormone in postmenopausal women with osteoporosis. J Clin Endocrinol Metab. 2006;91:1370–5.

40. Hodsman AB, Hanley DA, Ettinger MP, Bolognese MA, Fox J, Metcalfe AJ, Lindsay R. Efficacy and safety of human parathyroid hormone-(1–84) in increasing bone mineral density in postmenopausal osteoporosis. J Clin Endocrinol Metab. 2003;88:5212–20.

41. Kurland ES, Cosman F, McMahon DJ, Rosen CJ, Lindsay R, Bilezikian JP. Parathyroid hormone as a therapy for idiopathic osteoporosis in men: effects on bone mineral density and bone markers. J Clin Endocrinol Metab. 2000;85:3069–76.

42. Zanchetta JR, Bogado CE, Ferretti JL, Wang O, Wilson MG, Sato M, Gaich GA, Dalsky GP, Myers SL. Effects of teriparatide [recombinant human parathyroid hormone (1–34)] on cortical bone in postmenopausal women with osteoporosis. J Bone Miner Res. 2003;18:539–43.

43. Burr DB, Hirano T, Turner CH, Hotchkiss C, Brommage R, Hock JM. Intermittently administered human parathyroid hormone (1–34) treatment increases intracortical bone turnover and porosity without reducing bone strength in the humerus of ovariectomized cynomolgus monkeys. J Bone Miner Res. 2001;16:157–65.

44. Burr DB. Does early PTH treatment compromise bone strength? The balance between remodelling, porosity, bone mineral, and bone size. Curr Osteoporos Rep. 2005;3:19–24.

45. Jiang Y, Zhao JJ, Mitlak BH, Wang O, Genant HK, Eriksen EF. Recombinant human parathyroid hormone (1–34) [teriparatide] improves both cortical and cancellous bone structure. J Bone Miner Res. 2003;18:1932–41.

46. Black DM, Bilezikian JP, Ensrud KE, Greenspan SL, Palermo L, Hue T, Lang TF, McGowan JA, Rosen CJ. PaTH Study Investigators. One year of alendronate after one year of parathyroid hormone (1–84) for osteoporosis. N Engl J Med. 2005;353:555–65.

47. Blake GM, Park-Holohan SJ, Cook GJ, Fogelman I. Quantitative studies of bone with the use of 18F-fluoride and 99mTc-methylene diphosphonate. Semin Nucl Med. 2001;31:28–49.